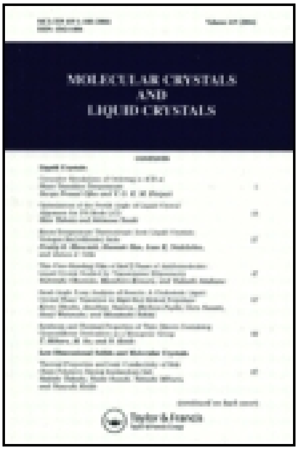

Molecular Crystals and Liquid Crystals Incorporating Nonlinear Optics

Publication details, including instructions for authors and subscription information:
http://www.tandfonline.com/loi/gmcl17

# Physical Properties of Schiff's Base Esters: n-Alkyl 4-[4′-(4″-n-octyloxybenzoyloxy)benzylidene] aminobenzoates

S. Lotke [a] & R. N. Patil [a]

[a] Department of Physics, Shivaji University, Kolhapur, 416 004, India

Version of record first published: 22 Sep 2006.

To cite this article: S. Lotke & R. N. Patil (1989): Physical Properties of Schiff's Base Esters: n-Alkyl 4-[4′-(4″-n-octyloxybenzoyloxy)benzylidene] aminobenzoates, Molecular Crystals and Liquid Crystals Incorporating Nonlinear Optics, 166:1, 43-60

To link to this article: http://dx.doi.org/10.1080/00268948908037137

*Mol. Cryst. Liq. Cryst.*, 1989, Vol. 166, pp. 43–60
Reprints available directly from the publisher
Photocopying permitted by license only

Printed in the United States of America

# Physical Properties of Schiff's Base Esters: *n*-Alkyl 4-[4′-(4″-*n*-octyloxybenzoyloxy)benzylidene] aminobenzoates

S. LOTKE and R. N. PATIL

*Department of Physics, Shivaji University,*
*Kolhapur 416 004, India.*

(*Received November 9, 1987; in final form February 5, 1988*)

A homologous series, *n*-alkyl 4-[4′-(4″-*n*-octyloxybenzoyloxy)benzylidene] aminobenzoates, exhibiting nematic (N), smectic A ($S_A$) and smectic C ($S_C$) trimorphism has been prepared. The liquid crystal behavior of the series is compared with that of a corresponding series, *n*-alkyl 4-[4′-(4″-*n*-octyloxybenzoyloxy)-3-methoxy benzylidene] aminobenzoates. The effect of a lateral methoxy substitution on mesomorphic properties of the series is discussed. Physical properties, such as, transition temperatures, transition heats, optical textures, densities, refractive indices and the orientational order parameter are studied. The $S_A$–$S_C$ phase transition is found to be second order. The $S_C$ phase appears to show a temperature dependent tilt angle. A binary phase diagram of one of the members of the series with terephthalylidene-bis-(4-*n*-butylaniline) (TBBA) is presented. It serves as an exception to the miscibility rule and also gives an induced smectic B phase.

## 1. INTRODUCTION

The geometrical aspects of a molecule play an important role in the establishment of liquid-crystalline properties in lath-like organic compounds. According to Gray,[1] the dipole moments acting across the long molecular axis may strongly favor smectic behavior and for this reason a compound with a terminal group such as ring —COOR would tend to be smectogenic. This remark seems to be in keeping with the earlier work of Dave and Patel[2] and Fishel and Patel.[3] Among the other important factors that promote the smectic character, the molecular length (especially, lengthening of the flexible alkyl chain) and intermolecular lateral cohesive forces, are worthy of consideration. Relatively few mesomorphic homologous series comprising of both an ester and an azomethine linkage in the same molecule seem to have been studied.[4–10] In continuation of our earlier work of investigating the mesomorphic behavior of compounds involving the —COOR end substitution in *para*-position to the —CH=N-linkage of the three phenylene ring system, we now report the mesomorphic properties of a homologous series, *n*-alkyl 4-[4′(4″-*n*-octyloxybenzoyloxy)benzylidene] aminobenzoates (series A), which has the general structure

I given below. The alkoxy substitution at one end of the molecule is confined to *X* = *n* − octyloxy in order to obtain comparatively low melting mesogens since the lower alkoxy substitutions resulted in mesogens with higher melting points. The present series exhibits nematic (N), smectic A ($S_A$), smectic C ($S_C$) trimorphism.

In this paper we report the transition temperatures, transition heats and optical textures of series A (structure I). A comparison is made of the mesomorphic properties of the series with those of an analogous series, *n*-alkyl 4-[4′(4″-*n*-octyloxybenzoyloxy)-3-methoxy benzylidene] aminobenzoates[11] (series B, structure II below). This enables us to investigate the effect of a lateral methoxy substitution on the mesomorphic character of the present series. We also report the temperature dependence of density (ρ), refractive indices ($n_e$, $n_o$), birefringence ($\Delta n$) and the microscopic order parameter (S) for two representative members of the series. A binary phase diagram is constructed in order to study the co-miscibility of N, $S_A$ and $S_C$ phases of the series with those of terephthalylidene-bis-(4-*n*-butylaniline) (TBBA).

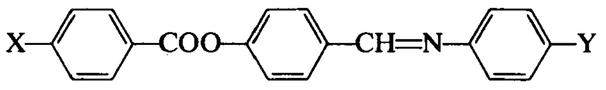

(I)

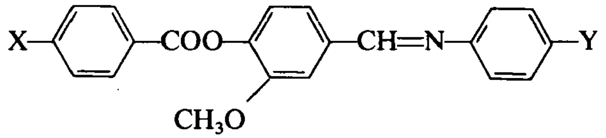

(II)

$X = OC_8H_{17}$;
$Y = COOC_nH_{2n+1}$, $n = 1$–$6$.

## 2. EXPERIMENTAL

### 2.1. Compound preparation

The Schiff's base esters were synthesized by condensing equimolar quantities of freshly prepared 4-(4′-*n*-octyloxybenzoyloxy) benzaldehyde[12] with the appropriate alkyl-*p*-aminobenzoates. The products were recrystallized from benzene-petroleum ether to constant transition temperatures. Structural identification of the compounds was made from their IR and NMR spectra.

### 2.2. Microscopy

Transition temperatures of the pure compounds given in (Table I), as well as in the admixed state (the miscibility study), were determined using a polarizing microscope equipped with a controlled microheating stage.

The microscopic slides and cover slips were treated overnight with freshly prepared chromic acid[13] and washed with distilled water. Using these slides homogeneous textures were observed. If on the other hand, the slides were cleaned by

TABLE I

*n*-Alkyl 4-[4′-(4″-*n*-octyloxybenzoyloxy)benzylidene] aminobenzoates

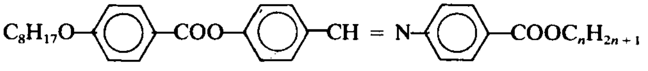

| Compound no. | *n* | | m.p. | C | | $S_C$ | | $S_A$ | | N | | I |
|---|---|---|---|---|---|---|---|---|---|---|---|---|
| A1 | 1 | (a) | 147 | · | 141 | — | | · | 224 | · | 261 | · |
| | | (b) | 7.12 | | | — | | · | 0.32 | · | 0.27 | · |
| | | (c) | 17.08 | | | — | | · | 0.64 | · | 0.51 | · |
| A2 | 2 | (a) | 148 | · | 140 | — | | · | 214 | · | 231 | · |
| | | (b) | 8.70 | | | — | | · | 0.42 | · | 0.20 | · |
| | | (c) | 20.97 | | | — | | · | 0.86 | · | 0.40 | · |
| A3 | 3 | (a) | 146.5 | · | 130 | — | | · | 212 | · | 224.5 | · |
| | | (b) | 10.59 | | | — | | · | 0.33 | · | 0.19 | · |
| | | (c) | 25.64 | | | — | | · | 0.69 | · | 0.39 | · |
| A4 | 4 | (a) | 126 | · | 112.5 | · | 142 | · | 203.5 | · | 207 | · |
| | | (b) | 9.75 | | | · | (d) | · | 0.60 | · | 0.23 | · |
| | | (c) | 24.86 | | | · | (d) | · | 1.27 | · | 0.47 | · |
| A5 | 5 | (a) | 132.5 | · | 125 | · | 137.5 | · | 208 | · | 211 | · |
| | | (b) | 9.85 | | | · | (d) | · | 0.64 | · | 0.22 | · |
| | | (c) | 24.75 | | | · | (d) | · | 1.34 | · | 0.46 | · |
| A6 | 6 | (a) | 126 | · | 120 | · | 152 | · | 195 | · | 196 | · |
| | | (b) | 11.40 | | | · | (d) | · | 1.24 | · | (e) | · |
| | | (c) | 29.00 | | | · | (d) | · | 2.66 | · | (e) | · |

(a) Transition temperatures (°C) according to the microscopic observation
(b) Transition enthalpy in K cal/mole
(c) Transition entropy in cal/mole/°K
(d) Absence of a latent heat at the $S_A/S_C$ transition
(e) N/I transition not resolved by DSC

placing them vertically in a liquid soap solution which was being heated from beneath, for an hour, and finally with distilled water, perfectly homeotropic textures were obtained using these slides. A texture showing both orientations (homogeneous as well as homeotropic) can be obtained by employing a suitable combination of the two treatments; Figure 1 gives such textures.

### 2.3. Calorimetry

Transition heats were determined using a Perkin–Elmer Differential Scanning Calorimeter DSC 2. Calibration of the apparatus was performed using tabulated heats of pure Indium. About 5–10 mg samples were used. A heating rate of 10°/min was employed. The areas under the DSC peaks were measured by planimetry and the transition heats were calculated. These are presented in Table I. The reproducibility of the DSC results was checked (discussed below, cf. 3.1).

### 2.4. Density and refractive indices

The capillary method was used for the density measurements and the refractive indices were measured by the hollow-prism method. Details regarding these measurements have been reported in our earlier paper.[14]

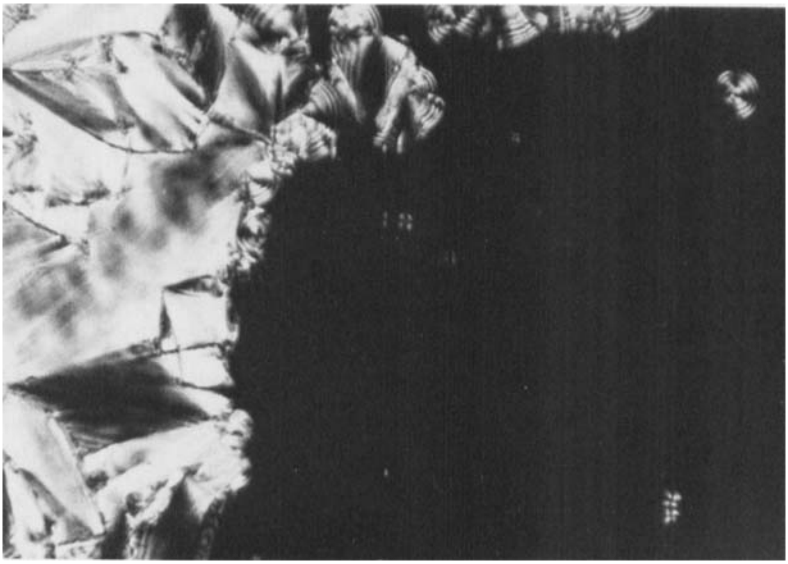

(a) See Color Plate I.

(b) See Color Plate II.

FIGURE 1 Microscopic textures (100 x) for A4, crossed polarizers (a) Focal-conic fan and homeotropic textures of $S_A$ phase, 175°C; (b) Broken focal-conic and *schlieren* textures of $S_C$ phase, 135°C; (c) *Ibid*, 120°C; (d) Solid state, 110°C.

(c) See Color Plate III.

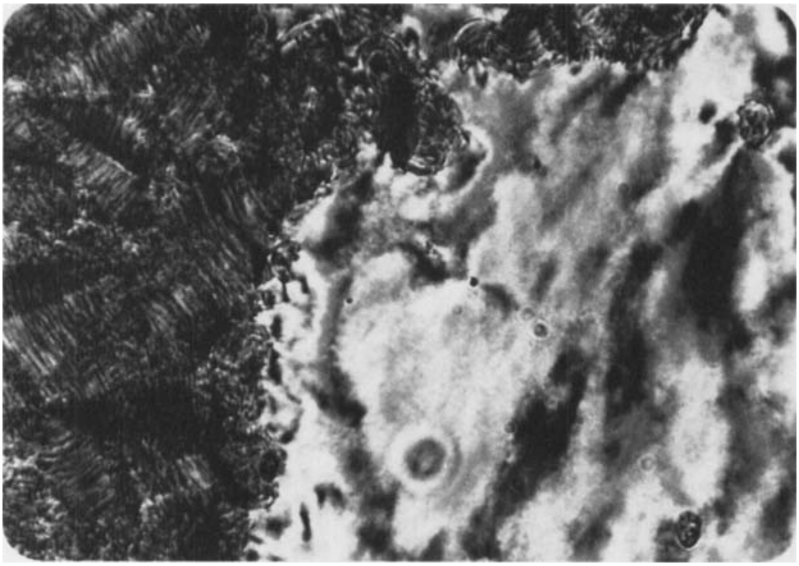

(d) See Color Plate IV.

FIGURE 1 (*Continued*)

## 3. RESULTS AND DISCUSSION

### 3.1. Liquid crystal behavior of series A

The very first member, A1, of the series exhibits polymorphism; it gives N and $S_A$ phases which are also present for the next two homologues, A2 and A3. Fourth member, A4, shows an additional smectic phase, *viz.* $S_C$, together with N and $S_A$ phases, but at the cost of considerable decrease in the temperature range of the N phase. All these phases are present in the fifth (A5) and sixth (A6) members; the N phase, however, is of only 1° interval in A6. These mesomorphic transitions are graphically presented in Figure 2. The usual odd–even effect of the N–I transitions is clearly seen. A similar trend is also followed by the N–$S_A$ transitions. The $S_A$–$S_C$ transitions, on the other hand, reflect an opposite trend, the even–odd effect. A similar effect is also shown by the $S_A$–$S_C$ transitions of the esters of

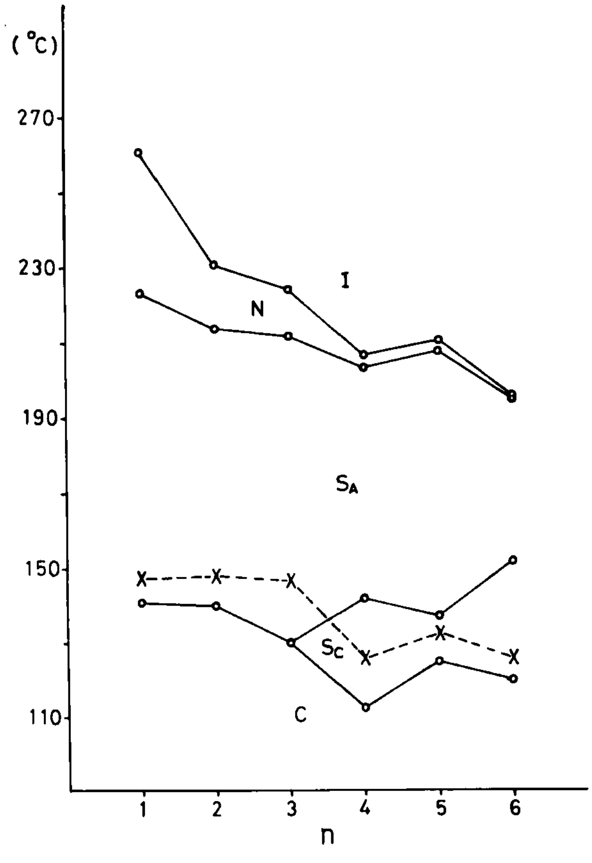

FIGURE 2 Transition temperatures (dotted line shows melting points) versus number of carbon atoms in the alkyl chain of *n*-alkyl 4-[4′-(4″-*n*-octyloxybenzoyloxy) benzylidene] aminobenzoates (series A).

4′-*n*-octyloxybiphenyl-4-carboxylic acid.[15] However, the data of transition temperatures of a few higher members of series A would be necessary to confirm this even–odd effect of the $S_A$–$S_C$ transitions.

McMillan's theory[16] predicts that when the molecular structure is dominated by two outboard dipoles that are approximately antiparallel and approximately perpendicular to the molecular long axis while the central dipoles (if any) do not show any special orientational relationship with the axis, the situation is favorable for the $S_C$ phase. The molecular structure of series A meets these requirements. Also, the structural studies made by de Jeu[17] point out that the introduction of an outboard dipole moment increases the tendency of the molecular species to form a $S_C$ phase. Therefore, McMillan's dipolar model appears to explain the occurrence of the $S_C$ phase in series A. It is, however, worth mentioning here that some of the esters with only a central dipole and no terminal dipoles are reported to exhibit $S_C$ phases.[18]

Characterization of the liquid-crystalline phases manifested by series A is made by observing their textures under the polarizing microscope. The homologues (A4–A6) of the series are found to exhibit smectic dimorphism. The microscopic preparations were made so as to give both homogeneous and homeotropic areas (cf. 2.2). Cooling the nematic phase of such a preparation results in a texture which is a combination of fan-shaped and optically extinguished (homeotropic) areas of $S_A$ phase. On cooling the $S_A$ phase, a transition to the $S_C$ phase takes place with the fans becoming broken and mottled in appearance, and the homeotropic areas become birefringent, exhibiting a *schlieren* texture. Both of these forms of the texture are typical[19] of the $S_C$ phase. Upon further cooling, the two areas crystallize to different solid state morphology. Figure 1 shows the microphotographs of these structural modifications for compound A4.

In $S_C$ phase the molecules are tilted with respect to the layer normal. The tilt angle of this phase in the present series appears to be temperature dependent[20] in view of the fact that the interference colors of the sample in the homeotropic region varied from near zero order at the $S_A$–$S_C$ transition to almost third order colors as the temperature approaches the solidification point and that the color changes are quite discontinuous. Two of these color changes are shown in Figure 1(b, c). If the microscopic preparation is reheated before allowing it to solidify the color changes reverse. The phenomenon is repetitive when the preparation is thermally oscillated in between the $S_C$–$S_A$ and $S_C$–C transition temperatures.

The DSC thermograms for A1 and A4 are presented in Figure 3, the dotted curves which (for A1) represent the transitions that are not repetitive, being observed only for the first heating run. Three such peaks are observed for A1, one relatively large for A2 and two comparatively small for A3. The sum total area under these peaks gradually reduces as the carbon number in the series increases and none of the higher members (A4–A6), which give an additional smectic phase, showed such behavior. The $S_A$–$S_C$ phase transition is not observed on the DSC thermograms for A4–A6 indicating that the phase change is a second-order phase transition. Also, that the tilt angle, a physical property, appears to be continuous at the phase transition, which is evidence that the phase transition is truly second order.

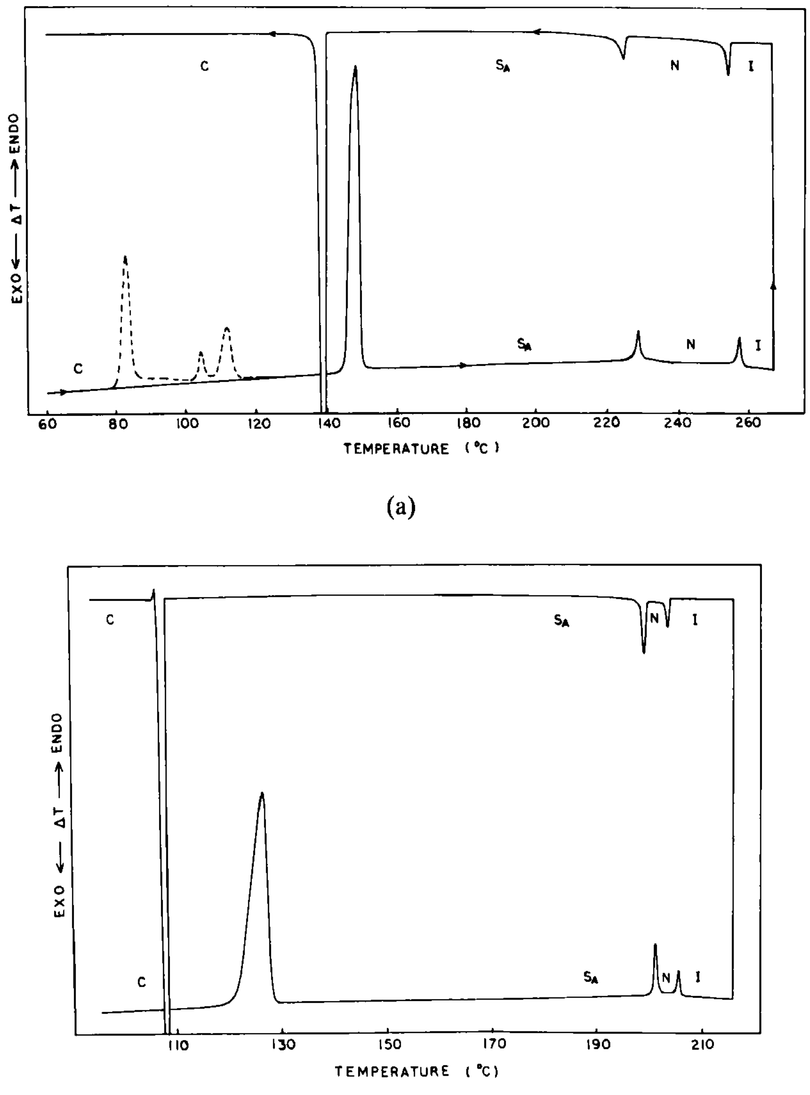

(a)

(b)

FIGURE 3 DSC thermograms obtained at a heating rate of 10°/min (a) Compound A1, (b) compound A4.

### 3.2. Comparison of mesomorphic character of series A and series B

Figure 4 represents a plot of mesomorphic transitions of series B. Comparison of the mesomorphic character of series A and series B yields: (i) Same trend is obeyed by the higher temperature (N–I) and the lower temperature (solidification) transitions in both the series. (ii) The temperature range of nematic phase increases as we approach lower *n* values in both the series, however, the extent of the increase is higher in series B. (iii) The fourth member in each series is a turning point in

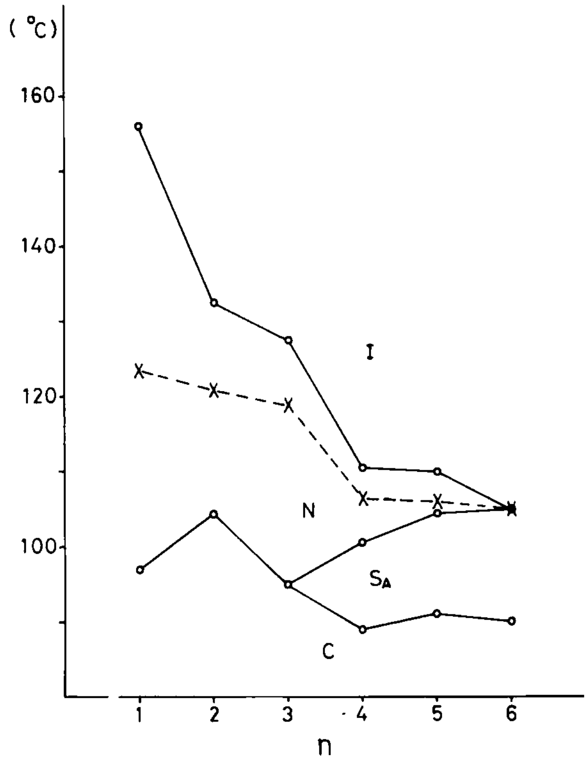

FIGURE 4 Transition temperatures (dotted line shows melting points) versus number of carbon atoms in the alkyl chain of *n*-alkyl 4-[4′-(4″-*n*-octyloxybenzoyloxy)-3-methoxy benzylidene] aminobenzoates (series B).

the mesomorphic character of the series; it gives an additional liquid-crystalline phase. (iv) Mesomorphic character of the sixth member is similar, again in both of the series in respect of the nematic phase, which, in series A lasts for only 1° temperature interval whereas in series B it is missing. (v) The $S_A$ phase shows alternate reduction in its temperature range in series A (so also does the $S_C$ phase) whereas it is gradually increasing in its temperature range in series B.

A plot of transition enthalpies is presented for both the series, Figure 5. It is seen that the curves representing the heat changes at the N–I transitions are more or less smooth for both of the series, whereas, the crystal-mesophase curve for series A is more regular than that for series B, the two curves crossing each other at a point wherefrom each of the two series exhibits a change in its mesomorphic behavior. $S_A$–N transition enthalpies for series A are much higher than those in series B and the N–I enthalpies in series A are slightly lower than those in series B.

### 3.3. Effect of lateral methoxy substitution

Lateral substituents like halogen or methyl reduce the crystal-mesophase transition temperatures quite effectively.[21,22] Recently some efforts have been made to study

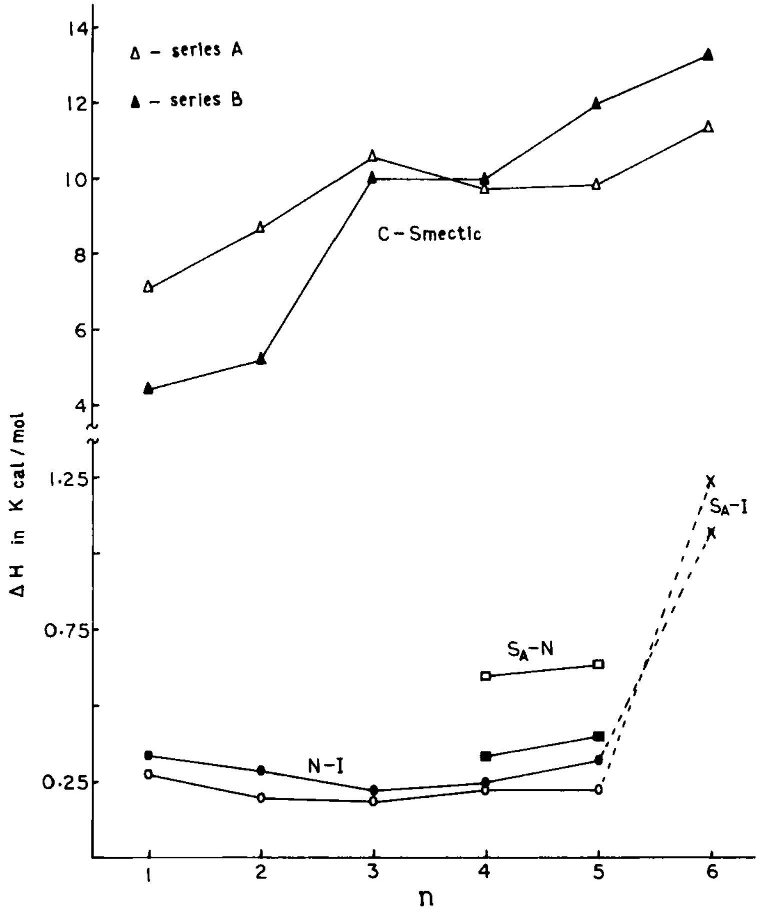

FIGURE 5 Transition enthalpy, ΔH, versus number of carbon atoms in the alkyl chain.

the effects of a bulky lateral methoxy substituent.[5,10,23,24] In the following we discuss the effects of lateral methoxy substituent on the mesomorphic character of series A and compare them with the known results.

The mesomorphic thermal stabilities of series B are much lower as compared to those of series A. Moreover, the smectic phase in series B is only monotropic in character as against the enantiotropism of all the liquid-crystalline phases exhibited by series A; and that series B lacks in $S_C$ modification. Both the series are structurally similar except the lateral methoxy group ortho to the ester linkage in series B. Because of this substitution in the lath-like molecule (structure I) the molecular geometry and anisotropy of molecular polarizability are seriously affected. Since the lateral substitution is in the central core part of the three ring system, steric effects, if any, are minimal. But the bulky substitution because of its bigger size increases breadth of the molecule, imposes greater intermolecular separation and reduces the coplanarity of the molecules. The substitution suppresses the rotational

TABLE II

Average thermal stabilities in °C

| | $S_A$ | N |
|---|---|---|
| Series A | 209.3 | 221.7 |
| Series B | 103.3 | 127.3 |

symmetry of the molecules about their long axis. Thermal stabilities of both the nematic and the smectic mesophases are affected. Table II summarizes average thermal stabilities of N and $S_A$ phases in the two cases.

Generally, introduction of lateral substitution renders a system low melting. But this is not the case with the lateral methoxy substitutions in the series studied by Vora and Gupta[5] and also by Gallardo and Silva,[10] so far as the first six members of those series are concerned. In the present work a comparatively large decrease in the melting point due to the lateral substitution is observed, the average decrease being 24.4°C. This, most probably, is because the —COOR terminal group also contributes to the broadening effect in addition to that due to the lateral substitution. The efficiency of the lateral substituent in lowering the clearing temperatures, however, remains of the same order in all the above series, the decrements lie in the range 80–105°C.

If we compare the nematic thermal stability of A1 with those of the octyloxy derivatives of series[4] (I; $Y = CH_3$ and $Y = OCH_3$) and similarly of B1 with those of the octyloxy derivatives of series[5] (II; $Y = CH_3$ and $Y = OCH_3$) we find that the order of efficiencies of the three terminal substituents in promoting nematic thermal stability is $COOCH_3 > OCH_3 > CH_3$. This order, thus, holds for both the laterally substituted and unsubstituted molecules of structure I. Moreover, comparison of the mesomorphism of these series[4,5] and also of the series[10] (I, II; $X = OC_7H_{15}$, $Y = OR$) with the present ones reveals that the —COOR terminal substitution indeed favors smectogenic character.

### 3.4. Density and refractive indices

A large amount of experimental work has been done over the last two decades to obtain the orientational order parameter using the density and refractive index data.[25-30] The temperature dependence of density for A3 and A4 is graphically presented in Figure 6(a) and (b) respectively. The density change at N–I and $S_A$–N transitions is noticeable, these being first order transitions; but there is practically no change in the slope of density curve at the $S_A$–$S_C$ transition which is second order. Figure 7(a) and (b) gives the temperature variation of the ordinary ($n_o$) and extraordinary ($n_e$) refractive indices and of the birefringence ($\Delta n$) of A3 and A4 respectively. The value of $n_o$ becomes constant throughout the smectic range except a small variation in the vicinity of $S_A$–N transition. On the other hand, $n_e$ varies over a large temperature interval but finally attains constant value for lower temperature region of the smectic phase. $\Delta n = (n_e - n_o)$, naturally, follows the trend of $n_e$.

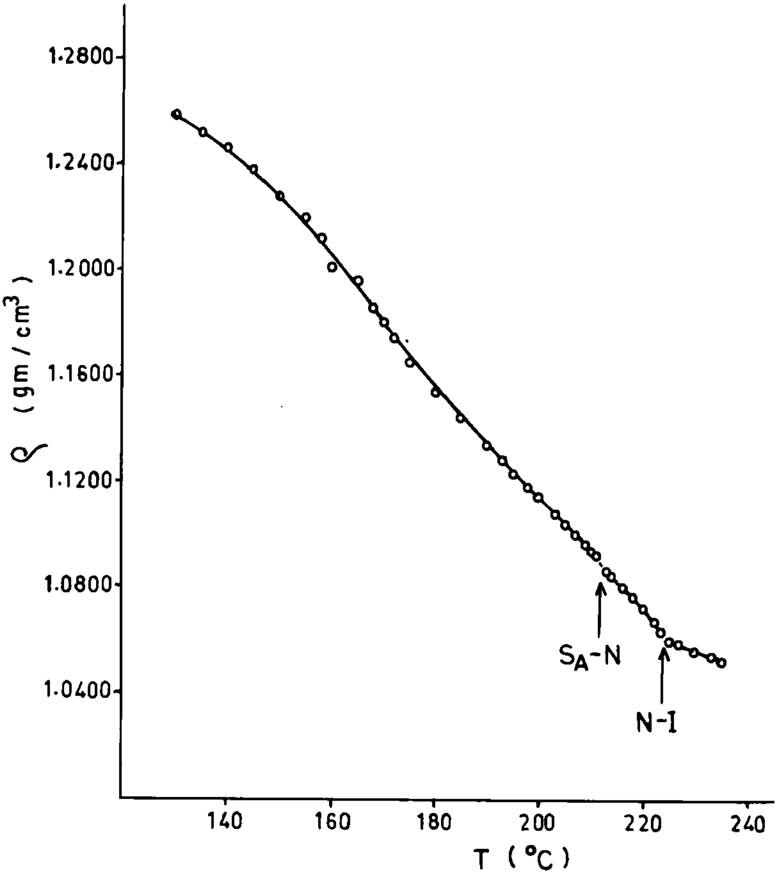

(a)

FIGURE 6 Variation of density with temperature for A3 (a) and A4 (b).

### 3.5. The order parameter

The orientational order parameter S is calculated by using the relation,

$$S = (\alpha_e - \alpha_o)/(\alpha_{\parallel} - \alpha_{\perp}),$$

where $\alpha_e$ and $\alpha_o$ are the average components of the molecular polarizability parallel and perpendicular to the optic axis and $\alpha_{\parallel}$ and $\alpha_{\perp}$ the molecular polarizabilities along the molecular axis and perpendicular to it. $\alpha_{e,o}$ are obtained using both Vuks and Neugebauer's relations.[31-34] According to Vuks approach, wherein the local field is assumed isotropic, the polarizabilities are given by

$$\alpha_{e,o} = \frac{3}{4\pi N} \cdot \frac{n_{e,o}^2 - 1}{\overline{n^2} + 2}$$

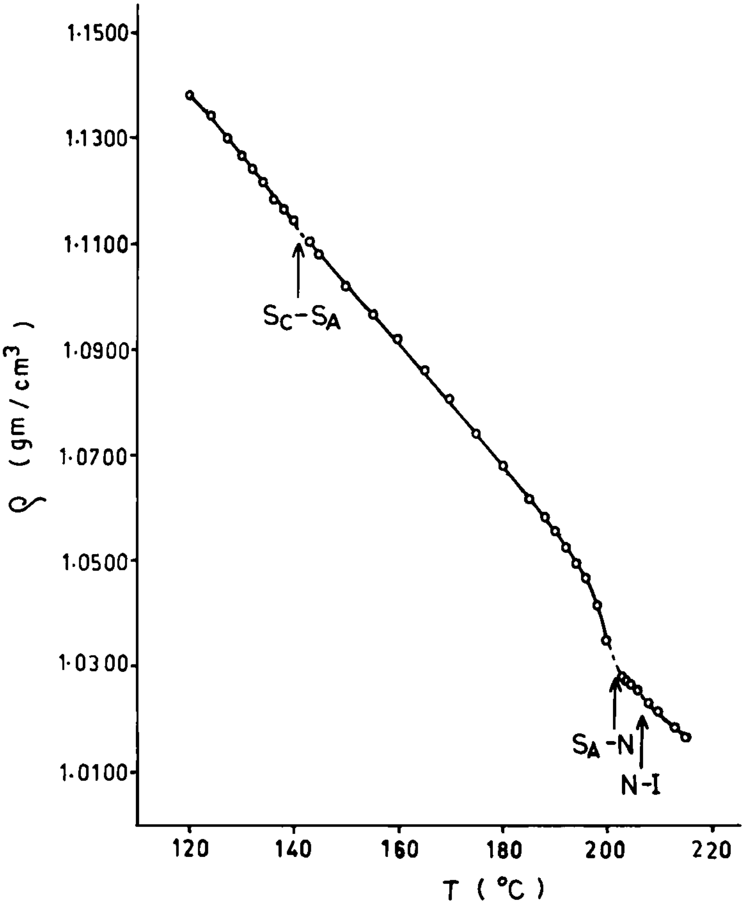

(b)

FIGURE 6 (*Continued*)

where $\overline{n^2} = n_e^2 + 2n_o^2)/3$ and $N = N_A\ \rho/M$, where $N_A$ is Avogadro's number, ρ the density and M is molecular weight. And, following Neugebauer's approach, assuming anisotropic nature of the local field, the polarizabilities are calculated using the relations,

$$\frac{1}{\alpha_e} + \frac{2}{\alpha_o} = \frac{4\pi N}{3}\left[\frac{n_e^2 + 2}{n_e^2 - 1} + 2\,\frac{n_o^2 + 2}{n_o^2 - 1}\right]$$

and

$$\alpha_e + 2\alpha_o = \frac{9}{4\pi N} \cdot \frac{\overline{n^2} - 1}{\overline{n^2} + 2}$$

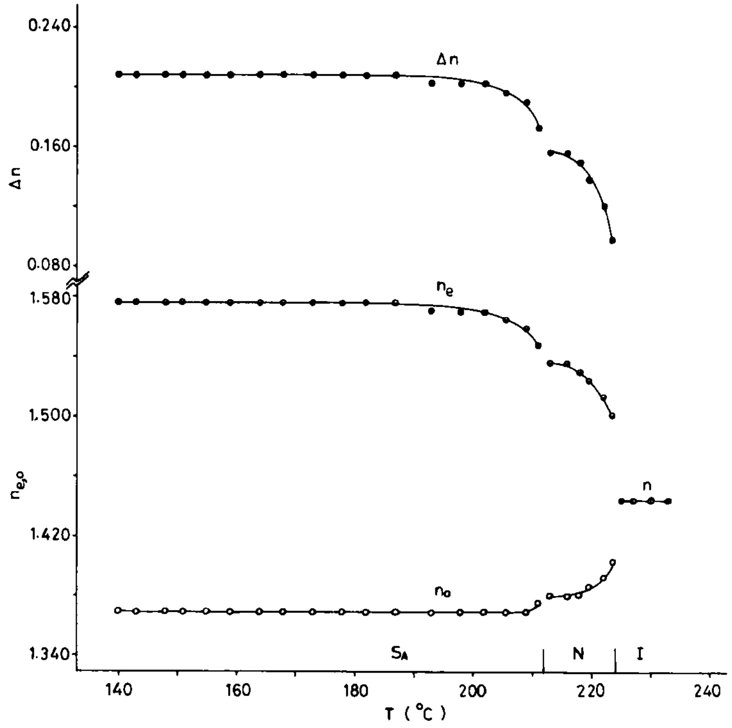

(a)

FIGURE 7 Temperature dependence of the refractive indices ($n_o$, $n_e$) and birefringence ($\Delta n$) of A3 (a) and A4 (b) for $\lambda$ = 5500 A°.

The value of $\alpha_{\parallel} - \alpha_{\perp}$ is obtained, as suggested by Haller *et al.*,[35] by extrapolating the linear portion of the log ($\alpha_e - \alpha_o$) vs log [(T − $T_c$)/$T_c$] curve in the nematic phase to T = 0°K.

The temperature variation of the order parameter S for A3 and A4 is shown in Figure 8(a) and (b) respectively for both Vuks and Neugebauer's approaches. S increases with decrease in temperature in the nematic phase in both the cases. In the case of A3 in the smectic phase S first increases with decrease in temperature, attains constant value for a small temperature interval and then decreases linearly to some extent for lower temperatures. The lowest value of S in the smectic phase is still much higher than its value in the nematic phase. The decrease of S is in accordance with the formulae used to calculate it wherein ρ keeps on increasing as temperature decreases while $n_{e,o}$ remain constant for lower temperatures. The same follows for S in the $S_C$ phase of A4. It is seen from the figure that the same trend is obeyed by S whether it is calculated by using Vuks or Neugebauer's approach and the S values are always higher in the latter case.

### 3.6. Miscibility study

A binary phase diagram is constructed in order to study the co-miscibility of the N, $S_A$ and $S_C$ phases of one of the members of the series (*viz.* A4) with TBBA

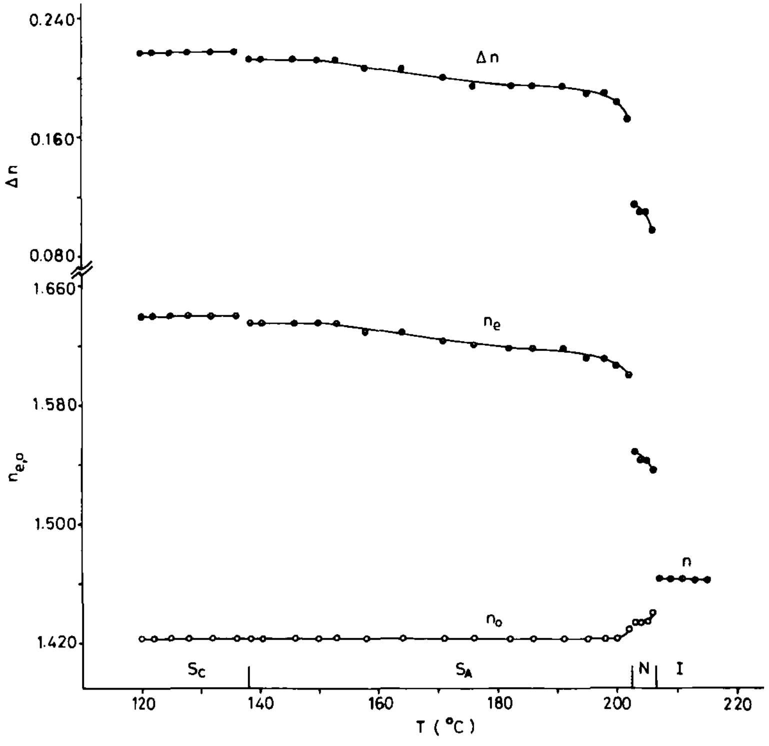

(b)

FIGURE 7 (*Continued*)

which also exhibits these three phases together with $S_G$ and $S_H$ phases.[36] The phase diagram is presented in Figure 9. The $S_C$ phase in each of the pure components is of the same type and in both of them it shows a temperature dependent tilt angle and so it is expected, in accordance with the rules of selective miscibility,[37] that this liquid-crystalline modification of A4 should be continuously miscible in all proportions with TBBA in the system. However, the system presents itself as an exception to the miscibility rules giving a composition range of 35–40% TBBA wherein the $S_C$ phase is not observed. Similar results about the absence of total miscibility of the same phase of each of the components are known.[38,39] A strong minimum in the miscibility curves of the $S_A$ phase is observed at 35% TBBA composition resulting in a eutectic point (temperature 88°C). These results may be attributed to the difference between the $S_C$ phases corresponding to the two components.

The miscibility results disclose that the admixed states are favorable for molecular associations which are characteristic of the $S_A$ phase type. The dominant role in this respect is played by the A4 molecules since the depression in the miscibility curve is to the A4 side and that the induced $S_B$ phase, characterized by the oc-

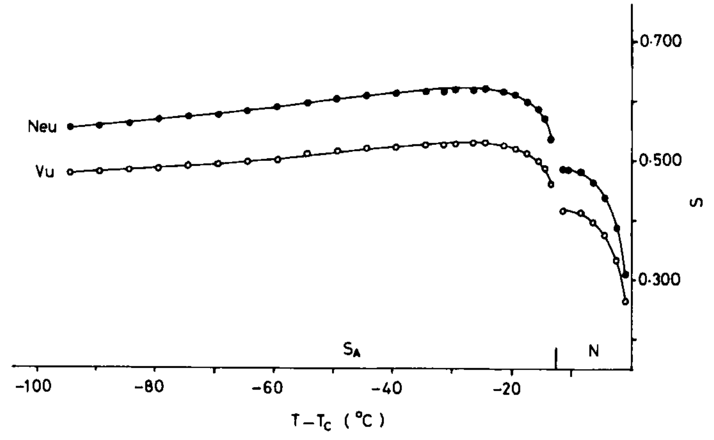

(a)

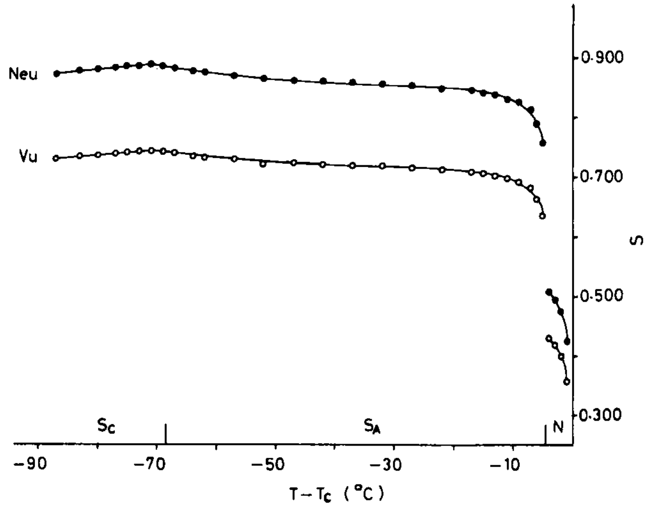

(b)

FIGURE 8 Variation of the order parameter $S$ with temperature for A3 (a) and A4 (b) calculated using Vuks and Neugebauer's approaches.

currence of transition bars, of the mixed crystals with 40, 50 and 60% TBBA composition exhibits a fan texture. Induced $S_B$ phases in the mixtures are often possible.[6,40,41] The phase diagram gives three triple points among the liquid-crystalline transitions. These are (i) $S_C$–$S_B$–$S_G$ at 117°C, (ii) $S_B$–$S_G$–$S_H$ at 108°C; these two in the vicinity of 70% TBBA composition, and (iii) $S_A$–$S_C$–$S_B$ at 93°C and 40% TBBA composition. The N and $S_A$ phases present total miscibility in the system.

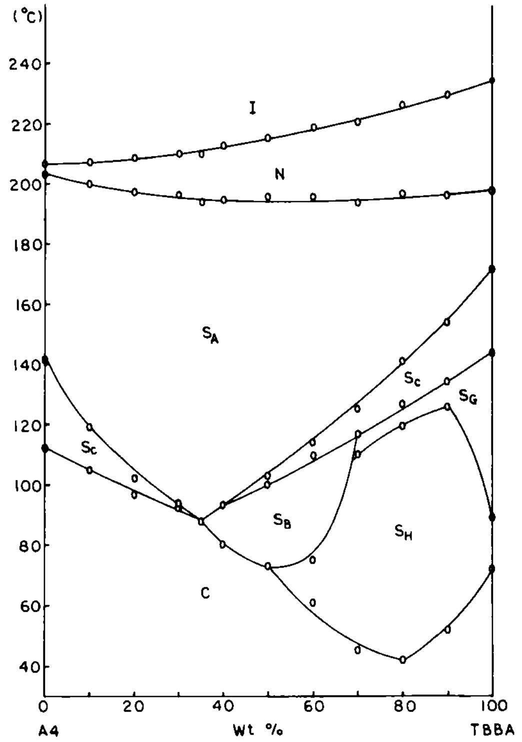

FIGURE 9 Diagram of state for mixtures (wt.%) of A4 and TBBA.

## Acknowledgments

The authors wish to thank Dr. J. R. Farnandes and I. S. Jarali (Indian Institute of Science, Bangalore) for their help in the DSC work.

## References

1. G. W. Gray, in *Liquid Crystals and Plastic Crystals*, Vol. 1 (G. W. Gray and P. A. Winsor, eds.), John Wiley and Sons, Inc., New York, 1974, Chap. 4.
2. J. S. Dave and P. R. Patel, *Molec. Crystals*, **2**, 103 (1966); see also: in *Liquid Crystals* (G. H. Brown, G. J. Dienes and M. M. Labes, eds.), Gordon and Breach, London, 1966, p. 375.
3. D. L. Fishel and P. R. Patel, *Mol. Cryst. Liq. Cryst.*, **17**, 139 (1972).
4. J. S. Dave and G. Kurian, ibid., **42**, 175 (1977).
5. R. A. Vora and Renu Gupta, ibid., **80**, 119 (1982).
6. W. Weissflog, G. Pelzl, A. Wiegeleben and D. Demus, *Mol. Cryst. Liq. Cryst. Lett.*, **56**, 295 (1980).
7. Nguyen Huu Tinh, A. Zann, J. C. Dubois and J. Billard, ibid., **56**, 323 (1980); ibid., **72**, 247 (1982).
8. Nguyen Huu Tinh, F. Hardouin, C. Destrade and H. Gasparoux, *J. Phys. Lett.*, **43**, 739 (1982).
9. S. Sakagami, *Bull. Chem. Soc. Jpn.*, **60**, 1153 (1987).
10. H. Gallardo and F. C. Silva, *J. Chem. Soc., Perkin Trans. II*, **3**, 320 (1987).
11. Satish Lotke and R. N. Patil, *Indian J. Chem.*, **25A**, 541 (1986).

12. J. S. Dave and G. Kurian, *J. dePhysique Coll.*, **C1**, 403 (1975).
13. A. I. Vogel, in *T. B. of Practical Organic Chemistry*, 3rd Edn., ELBS and Longman, London, 1968, Chap. II, p. 53.
14. S. D. Lotke, S. B. Desai and R. N. Patil, *Mol. Cryst. Liq. Cryst.*, **99**, 267 (1983).
15. J. W. Goodby and G. W. Gray, *ibid.*, **48**, 127 (1978).
16. W. L. McMillan, *Phys. Rev. A*, **8**, 1921 (1973).
17. W. H. deJeu, *J. Phys.* (*Paris*), **38**, 1265 (1977).
18. J. W. Goodby, G. W. Gray and D. G. McDonnell, *Mol. Cryst. Liq. Cryst. Lett.*, **34**, 183 (1977).
19. J. W. Goodby, T. M. Leslie, P. E. Cladis and P. L. Finn, in *Liquid Crystals and Ordered Fluids*, Vol. 4 (A. C. Giffin and J. F. Johnson, eds.), Plenum Press, New York, 1984, p. 89.
20. T. R. Taylor, S. L. Arora and J. L. Fergason, *Phys. Rev. Lett.*, **25**, 722 (1970).
21. S. L. Arora, J. L. Fergason and A. Saupe, *Mol. Cryst. Liq. Cryst.*, **10**, 243 (1970).
22. Z. G. Gardlund, R. J. Curtis and G. W. Smith, in *Liquid Crystals and Ordered Fluids*, Vol. 2 (J. F. Johnson and R. S. Porter, eds.), Plenum Press, New York, 1979, p. 541.
23. B. K. Sadashiva, *Mol. Cryst. Liq. Cryst.*, **110**, 309 (1984).
24. M. Subramanya Raj Urs and V. Surendranath, *ibid.*, **99**, 279 (1983).
25. S. Chandrasekhar and N. V. Madhusudana, *J. de Physique Coll.*, **C4**, 24 (1969).
26. J. Shashidhara Prasad and H. S. Subramhanyam, *Mol. Cryst. Liq. Cryst.*, **33**, 77 (1976).
27. R. G. Horn, *J. de Physique*, **39**, 105 (1978).
28. R. K. Sarna and V. G. Bhide, *Mol. Cryst. Liq. Cryst.*, **88**, 65 (1982).
29. S. Sen, K. Kali, S. K. Roy and S. B. Roy, *ibid.*, **126**, 269 (1985).
30. N. V. S. Rao, V. G. K. M. Pisipati, P. V. D. Prasad and P. R. Alapati, *ibid.*, **132**, 1 (1986).
31. M. F. Vuks, *Opt. and Spectros.*, **20**, 361 (1966).
32. H. E. J. Neugebauer, *Can. J. Phys.*, **32**, 1 (1954).
33. R. K. Sarna, B. Bahadur and V. G. Bhide, *Mol. Cryst. Liq. Cryst.*, **51**, 117 (1979).
34. D. Krishnamurti and R. Somashekar, *ibid.*, **75**, 133 (1981).
35. I. Haller, H. A. Huggins, H. R. Lilienthal and T. R. McGuire, *J. Phys. Chem.*, **77**, 950 (1973).
36. L. Richter, D. Demus and H. Sackmann, *Mol. Cryst. Liq. Cryst.*, **71**, 269 (1981).
37. H. Sackmann and D. Demus, *ibid.*, **21**, 239 (1973).
38. H. Sackmann and D. Demus, *Z. phys. Chem.* (*Leipzig*), **222**, 143 (1963).
39. N. K. Sharma, R. K. Bamezai, *J. Indian Chem. Soc.*, **61**, 667 (1984).
40. N. K. Sharma and R. K. Bamezai, *Indian J. Chem., Sect. A*, **25A**, 431 (1986).
41. G. Pelzl, M. Novak, W. Weissflog and D. Demus, *Cryst. Res. Technol.*, **22**, K 125 (1987).